

Dynamics and limitations of spontaneous polyelectrolyte intrusion into a charged nanocavity

Qianqian Cao^{1,2,*} and Michael Bachmann^{1,3,4,†}

¹*Soft Matter Systems Research Group, Center for Simulational Physics, The University of Georgia, Athens, Georgia 30602, USA*

²*Institut für Theoretische Physik, Freie Universität Berlin, Arnimallee 14, 14195 Berlin, Germany*

³*Instituto de Física, Universidade Federal de Mato Grosso, 78060-900 Cuiabá, Mato Grosso, Brazil*

⁴*Departamento de Física, Universidade Federal de Minas Gerais, 31270-901 Belo Horizonte, Minas Gerais, Brazil*

(Received 11 April 2014; revised manuscript received 4 November 2014; published 30 December 2014)

We systematically investigate the spontaneous packaging mechanism of a single polyelectrolyte chain into an oppositely charged nanocavity by Langevin molecular dynamics simulations of a generic coarse-grained model. Intrusion dynamics and packaging rate, as well as the self-assembly process inside turn out to depend sensitively on the stiffness of the polyelectrolyte, the surface charge density inside the capsid, and the radius of the cavity. Further analysis shows that, depending on the stiffness, thermal fluctuations and charge inversion can be important factors to overcome barriers that slow down the intrusion and packaging dynamics. These results help advance our understanding of the function of charges on the inner surface of viral capsids and the possibility to design capsids as synthetic nanocarriers.

DOI: [10.1103/PhysRevE.90.060601](https://doi.org/10.1103/PhysRevE.90.060601)

PACS number(s): 82.35.Rs, 64.75.-g, 82.35.Lr, 87.15.-v

In recent years, there has been an increasing interest in studies of polymer conformations in confined spaces. Quite naturally, particular attention has been dedicated to genome confinement and packaging in viruses [1–6] and viral assembly [7–16]. Other topics included confinement-induced crystallization of polymers [17], translocation of DNA through nanopores [18], and adsorption and assembly near attractive surfaces [19,20] and soft nanoparticles [21]. Confinement effectively reduces translational and conformational entropy. For semiflexible polymers, this is unfavorable if the characteristic length scale of the confined space is smaller than the persistence length of the chain. To mention an example, double-stranded (ds) DNA with a persistence length of about 50 nm is subject to high energetic and entropic penalties to fit within a small viral capsid with a diameter of similar scale (e.g., in the case of the adenovirus). Since the polyelectrolyte is forced to form energetically unfavorable conformations, tightly packed DNA or RNA in a capsid exerts a high pressure onto the capsid shell [22]. This pressure is necessary for the injection of the viral DNA or RNA into cells.

Understanding how polymer structures emerge under thermal conditions [23] and are forced to persist in confined environments is a key problem in biophysics and it is also relevant for potential nanotechnological applications. The packaging of many viral genomes is accomplished by a powerful ATP-driven motor [1]. In addition, also other mechanisms to drive polymers into confined spaces are known, e.g., by external fields and proteins that help neutralize repulsion by like charges. Electric fields enable the translocation of single molecules through nanometer-sized pores and are used *in vitro* for the detection and analysis of biomolecules [18,24]. The migration of polymers by translocation of DNA through membranes can be driven by means of chaperons [25]. These mechanisms have also been studied theoretically [26–29].

In this Rapid Communication, we turn around the problem of viral assembly and genome confinement and investigate

the conditions for polyelectrolytes to intrude into an already assembled cavity *spontaneously*. The answers we get from the simulations of a simplified, coarse-grained model, which reveal the substantial limitations of a spontaneous intrusion process make quite clear why such a process has not been considered an option in viral evolution. However, from a technological perspective of synthetic nanocontainer design, it is of interest that these processes are possible, in principle, within the limits discussed in the following. This problem has not yet been addressed systematically.

Most studies either focus on the motor-assisted packaging dynamics [12,30] or discuss structural features of polyelectrolytes confined in charged capsids [10,31] or neutral polymers inside attractive cavities [32]. However, our approach enables us to determine the dynamic properties and the equilibrium conditions of polymer structures in an open cavity by systematically varying the polymer stiffness, as well as the radius and charge density of the inner shell of the nanocavity. Experimentally, it is difficult to determine the influence of surface charges inside the cavity upon the packaging process. Therefore, predictive computational studies help to better understand the stability conditions of spontaneous polyelectrolyte packaging.

In our study, the cationic polyelectrolyte is represented by a generic coarse-grained bead-spring polymer chain, consisting of $N_p = 200$ beads with diameter $\sigma = 2$ nm (which, for comparison, is about the nominal diameter of dsDNA). The spherical cavity with inner radius R_{in} is enclosed by a shell of thickness 3σ . The cavity possesses a portal tube with radius 1.5σ that enables the polyelectrolyte that initially resides outside to intrude into the cavity. The cavity hull, which consists of an inner and an outer wall, is permeable to counterions, but impermeable to the polyelectrolyte. The outer wall is neutral. In the inner shell, N_c positively charged particles are uniformly distributed. The average charge density is given by $\alpha = N_c/N_i$, where N_i is the total number of particles in this shell.

The short-range excluded volume interactions between monomers of the polyelectrolyte are modeled by the repulsive part of the Lennard-Jones (LJ) potential with interaction

*qqcao@physik.fu-berlin.de

†bachmann@smsyslab.org; <http://www.smsyslab.org>

strength $\epsilon_{LJ} = k_B T$, where k_B is the Boltzmann constant and $T = 300$ K is the temperature. The LJ potential is truncated and shifted at the cutoff distance $r_c = 2^{1/6}\sigma$. The interaction between bonded monomers is described by a finitely extensible nonlinear elastic potential with a maximum bond length $R_0 = 1.5\sigma$ and a spring constant $k_l = 30\epsilon_{LJ}/\sigma^2$ [33]. Resistance against bending is taken into account by a harmonic potential of the bending angle θ . In separate simulations, we vary the bond stiffness in units of $k_\theta^* = \epsilon_{LJ}/\text{rad}^2$ from $k_\theta = 0$ (for a flexible chain) to $300k_\theta^*$ (approximately the stiffness of dsDNA in the low salt concentration limit). Coulomb forces between charged particles are calculated using the particle-particle-particle-mesh (PPPM) algorithm [34]. In the PPPM method the charges are mapped on a three-dimensional mesh and fast Fourier transforms are used to solve the discrete Poisson equation on the mesh. The electric field at the particle's position is calculated by interpolating the mesh based electric field.

The Bjerrum length $\lambda_B = e^2/(4\pi\epsilon_0\epsilon_r k_B T)$, where ϵ_0 and ϵ_r are the vacuum permittivity and the dielectric constant of solvent, respectively, is set to σ . The capsid geometry is considered rigid.

We employed the Large-Scale Atomic/Molecular Massively Parallel Simulator [35] to perform Langevin thermostatted molecular dynamics simulations [36] in a periodic cubic simulation box of edge length $L = 250\sigma$. Initially, neutralizing counterions (N_p anions and N_c cations) are randomly dispersed within the simulation box, and one end of the polyelectrolyte is located inside the portal region of the capsid shell. In our model, the LJ parameters ϵ_{LJ} and σ set the basic energy and length scales, respectively, and masses scale with the bead mass m . These constants fix the time scale, $\tau = (m\sigma^2/\epsilon_{LJ})$. For a polyelectrolyte such as dsDNA, this corresponds to $\tau \approx 79$ ps. In our simulations, each time step represented 0.008τ and the maximum number of time steps was 10^7 . Each simulation was repeated five times in order to verify consistency.

As a first major result, Fig. 1(a) shows the spontaneous packaging fraction χ , i.e., the relative number of packed monomers inside the capsid, as a function of time at $\alpha = 0.8$ and $R_{in} = 7\sigma$ for four values of the chain stiffness k_θ . The graphs clearly indicate the competition between the attractive electrostatic forces that pull the polyelectrolyte into the capsid and the resistance of semiflexible chains against dense packing inside the capsid. Whereas the flexible chain ($k_\theta = 0$) is accommodated in a quick, almost continuous process, the intrusion dynamics slows down for stiffer chains, and for chains with stiffness $k_\theta \gtrsim 200k_\theta^*$ it stops once a critical monomer density is reached in the interior of the cavity. As the inset in Fig. 1(a) shows, monomers of stiffer polyelectrolytes assemble close to the inner surface by reducing monomer-monomer contacts in favor of monomer-surface contacts.

From investigations of motor controlled packing dynamics of semiflexible polymers, it is known that pauses occur due to polymer rearrangement inside the cavity [30]. The motor is needed to provide the energy to overcome this type of solid-solid transition inside the capsid. Without motor assistance, this process can occur spontaneously only on very large time scales. The sensitive dependence of the packaging fraction on

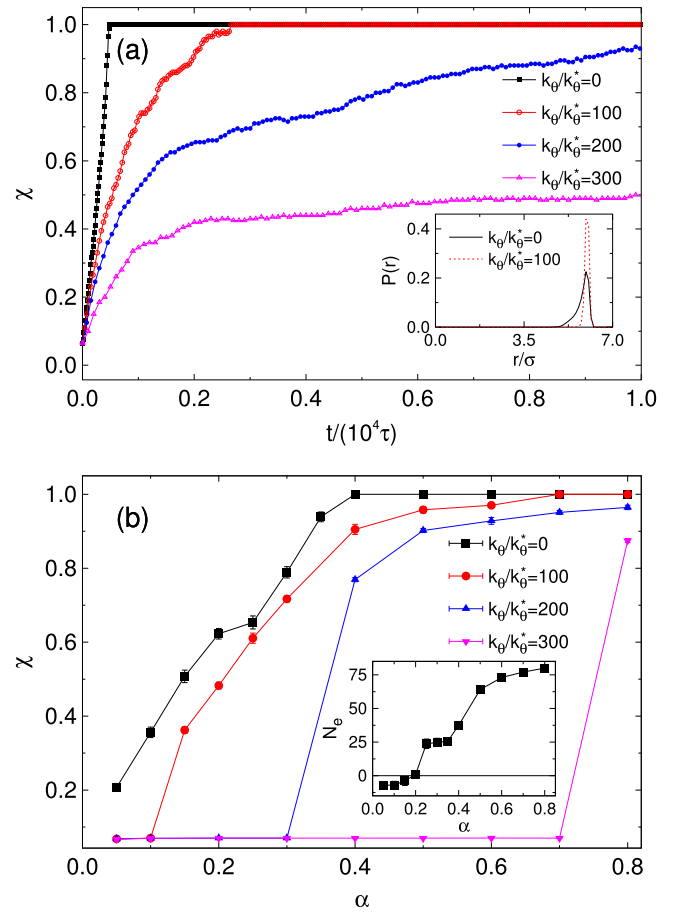


FIG. 1. (Color online) (a) Representative trajectories of the packaging fraction χ at charge density $\alpha = 0.8$ for a linear polyelectrolyte with $N_p = 200$ monomers. The distribution of polyelectrolyte monomers from the center of the cavity is plotted in the inset for $k_\theta = 0$ and $k_\theta = 100k_\theta^*$ at $\alpha = 0.8$. (b) χ as a function of α for different values of chain stiffness (averaged over five independent simulations). The inset shows for the flexible polymer ($k_\theta = 0$) the net charge $N_e = -N_p\chi + N_c + N_{pi} - N_{ci}$, where $N_{pi,ci}$ are the numbers of anionic and cationic counterions inside and adsorbed to the outer capsid hull, as a function of α . Charge inversion inside the cavity occurs for $\alpha > 0.2$. The capsid radius is $R_{in} = 7\sigma$.

the surface charge density is plotted in Fig. 1(b) for different bending stiffnesses. Unless the chain is flexible, it requires a substantial surface charge density inside the cavity to initiate the polyelectrolyte inclusion process. However, if α exceeds a threshold value that depends on the chain stiffness, the chain spontaneously intrudes into the capsid, but it requires statistical fluctuations to pass the metastable state that hinders the intrusion process.

Note that the flexible polymer can only be completely accommodated inside the cavity if the cavity is noticeably positively overcharged [see the inset in Fig. 1(b)]. Additional cations accompany the polymer into the cavity or adsorb on the outside shell of the capsid. However, no anions enter the capsid and, therefore, the tight packing of the polyelectrolyte is not induced by counterion condensation. If the number of surface charges is too small ($\alpha < 0.4$), the polyelectrolyte does not intrude entirely. Below $\alpha < 0.2$, the capsid gets negatively

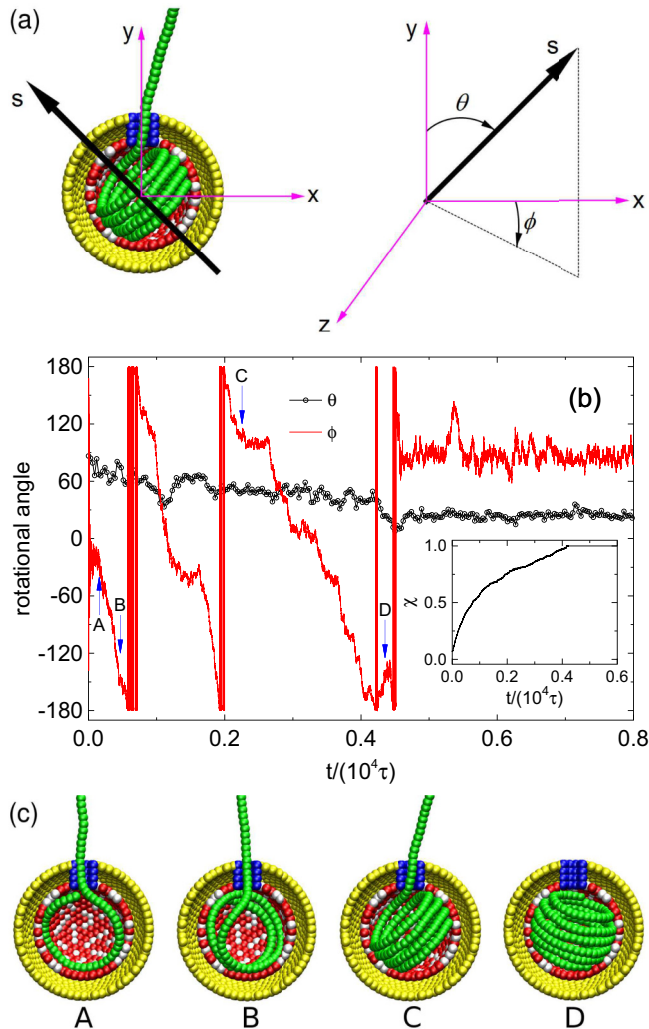


FIG. 2. (Color online) (a) Definition of the director axis s and the spherical angles θ and ϕ for a spool-like polyelectrolyte structure in a Cartesian coordinate system, where the y axis coincides with the direction of the portal tube of the capsid. The coordinate origin is located at the center of the cavity. (b) Time evolution of θ and ϕ at stiffness $k_\theta = 100k_\theta^*$, charge density $\alpha = 0.7$, and capsid radius $R_{\text{in}} = 7\sigma$ for a single intrusion event. The inset shows the time evolution of the packaging fraction $\chi(t)$. (c) Snapshots corresponding to A–D in (b). Counterions are not shown.

overcharged, which also leads to a stop of the intrusion process due to electrostatic repulsion between intruding and already packed monomers. The counterion distributions and the necessity of charge inversion are discussed in more detail in the Supplemental Material [37].

The structural in-depth analysis in Fig. 2 reveals how the semiflexible polymer with a stiffness below the critical threshold completely accommodates itself inside the capsid, where it finally adopts a well-defined spool-like, helical conformation. For the subsequent discussion, it is useful to introduce the polar and azimuthal angles θ and ϕ , respectively, of the director axis s of the helical spool in a Cartesian coordinate system, in which the y axis points along the tube axis of the cavity. This is schematically shown in Fig. 2(a). The rotational dynamics of θ and ϕ are plotted in Fig. 2(b) for a

semiflexible polyelectrolyte with bending stiffness $k_\theta = 100k_\theta^*$ at capsid surface charge density $\alpha = 0.7$ and capsid radius $R_{\text{in}} = 7\sigma$. As discussed earlier, this parametrization allows for the spontaneous inclusion of the entire chain into the capsid.

In the early stages, the chain end that enters the capsid first forms a ringlike conformation with maximum possible radius, and the director s points almost perpendicular to the portal tube axis ($\theta \approx 90^\circ$). The corresponding structure (A) is shown in Fig. 2(c). Then the plane formed by the area of the ring tilts ($\theta \approx 70^\circ$) in order to make space for the monomers that fill the second winding. The first ring is displaced out of the center and slightly compressed. The director of the already included segment rotates about the tube axis almost continuously, while more monomers enter the cavity. A second winding forms (B). The rotation process is necessary to avoid additional bending strain on the following chain segment intruding into the capsid. The tilting angle of the plane perpendicular to s remains relatively stable at about $\theta \approx 60^\circ$. However, the more windings are added to the spool the more difficult it becomes for the polyelectrolyte to minimize the strain by bending. The available space inside the capsid becomes so small whenever a winding is completed that the bending angle with the following, still almost straight, segment in the tube is so large that the further insertion of monomers into the cavity does not lead to an energetically more favorable conformation. The inclusion process stops or pauses and it requires a thermal fluctuation to overcome the energetic bending barrier. A structure that is representative at such a transition point is shown in Fig. 2(c). If the bending “penalty” is larger than the available free energy, as this is, for example, the case for $k_\theta \gtrsim 200k_\theta^*$, the entire process stops and remains in a metastable state for a very long period of time. In the example described here, the process is completed (D) and after a short period of fluctuations necessary to optimize the global adaptation to the disordered environment of the surface charges inside the capsid, the rotation stops. The polyelectrolyte is finally safely packaged in the cavity. The dynamics of energies and forces for this successful intrusion process is analyzed in the Supplemental Material [37].

It is obvious that the radius of the cavity is an essential parameter that influences the spontaneous packaging capability of the polyelectrolyte. Figure 3 shows the dynamics of packaging for (a) the entirely flexible chain ($k_\theta = 0$) and (b) an example for a semiflexible polyelectrolyte with $k_\theta = 200k_\theta^*$ for four values of the inner cavity radius R_{in} and constant number of surface charges in the cavity ($N_c = 315$). Except for the smallest radius $R_{\text{in}} = 5\sigma$, in which case the interior volume is simply too small to accommodate all monomers, the intrusion of the flexible polyelectrolyte into the cavity is a quick and almost linear process, i.e., no pauses occur [Fig. 3(a)]. Monomer intrusion and rearrangement inside the cavity are simultaneous, cooperative processes. It has been found previously [38] that an entropic springlike release of the flexible polymer can occur if the polymer cannot be accommodated in the capsid. Because of the strong electrostatic forces inside the capsid and the rather short tail that remains outside, we do not observe such an effect for $R_{\text{in}} = 5\sigma$. However, in first simulations of longer chains (with up to 900 beads) we find that such a behavior can occur.

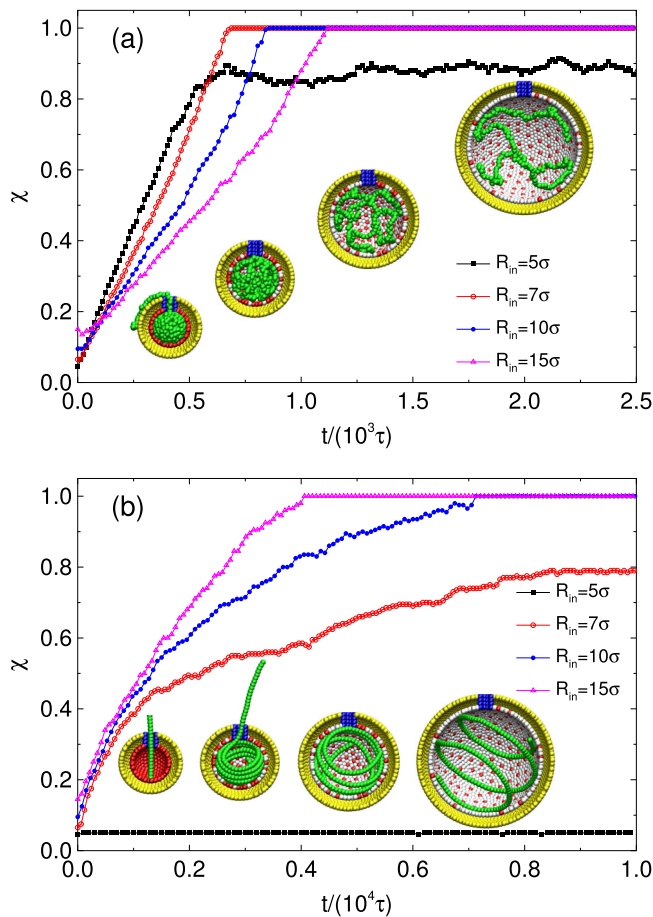


FIG. 3. (Color online) Time evolution of packaging fraction for (a) the flexible ($k_\theta = 0$) and (b) a semiflexible polyelectrolyte ($k_\theta = 200k_\theta^*$) at various cavity radii. The snapshots represent typical polymer conformations. In all cases, the number of surface charges is kept constant, $N_c = 315$.

The situation is completely different for a semiflexible polymer. As Fig. 3(b) shows, any packaging is impossible, if the radius is too small compared to the persistence length of the polyelectrolyte ($R_{in} = 5\sigma$). Even the initial stage of the packaging process as described above—the formation of a ringlike conformation—is not possible. No bending occurs. Accompanied by several pauses, the situation improves for $R_{in} = 7\sigma$, but the intrusion comes to an early end when bending forces and attractive nonbonded and electrostatic

forces balance each other before all monomers could enter the cavity. The inclusion dynamics slows down exponentially and includes pauses for $R_{in} = 10\sigma$, but the majority of the monomers finds their place inside the cavity and the few remaining ones are accommodated by a favorable fluctuation. For the parameters chosen, $R_{in} \approx 10\sigma$ represents the threshold radius for successful inclusion of the entire chain. For radii $R_{in} > 10\sigma$, the process is straightforward. However, although almost no pauses occur, the process is not linear. As the comparison of Figs. 3(a) and 3(b) also shows, the packaging speed of a flexible chain is faster the smaller the cavity is, but for the semiflexible example the opposite holds. This is plausible as in the flexible case already intruded densely packed monomers and counterions cooperatively assist in pulling in more monomers, which is different for semiflexible chains because of the increased bending effects that act anticooperatively upon not yet intruded monomers.

To summarize, we found that intrusion and packaging are highly cooperative processes for flexible chains, as long as the surface charge density inside the cavity and the cavity radius are sufficiently large. The dynamics is completely different for semiflexible polymers and it is accompanied by significant pauses in metastable states. It requires thermal fluctuations to reinitiate the inclusion process. If the energetic barriers are too large (because of too low surface charge density, too large bending stiffness, or too small cavity radius), the inclusion process cannot be completed on reasonable time scales. For flexible chains, it turns out that charge inversion inside the capsid is necessary to complete the intrusion process, provided the surface charge density of the interior wall of the cavity is sufficiently large. We also find that no anions participate in the intrusion process, i.e., the tight packing of the polyelectrolyte inside is not caused by counterion condensation.

The systematic computational study that we performed for a generic model enables the nonempirical approach to the technological design of nanocarriers for the transport of molecular substances. Furthermore, our study reveals the limits of spontaneous polyelectrolyte packaging in a capsid which consolidates the necessity of motor support in viral capsids [39].

We thank Hao You and Kai Qi for useful discussions. Q.C. gratefully acknowledges support by the Alexander von Humboldt Foundation. This work has been supported partially by the NSF under Grant No. DMR-1207437 and by CNPq (National Council for Scientific and Technological Development, Brazil) under Grant No. 402091/2012-4.

- [1] D. E. Smith, S. J. Tans, S. B. Smith, S. Grimes, D. L. Anderson, and C. Bustamante, *Nature (London)* **413**, 748 (2001).
- [2] V. A. Belyi and M. Muthukumar, *Proc. Natl. Acad. Sci. USA* **103**, 17174 (2006).
- [3] A. Matsuyama, M. Yano, and A. Matsuda, *J. Chem. Phys.* **131**, 105104 (2009).
- [4] Q. M. Elrad and M. F. Hagan, *Phys. Biol.* **7**, 045003 (2010).
- [5] J. A. Speir and J. E. Johnson, *Curr. Opin. Struct. Biol.* **22**, 65 (2012).
- [6] A. Al Lawati, I. Ali, and M. Al Barwani, *PLoS One* **8**, e52958 (2013).
- [7] S. C. Harvey, A. S. Petrov, B. Devkota, and M. B. Boz, *Phys. Chem. Chem. Phys.* **11**, 10553 (2009).
- [8] J. Rong, Z. Niu, L. A. Lee, and Q. Wang, *Curr. Opin. Colloid Interface Sci.* **16**, 441 (2011).
- [9] T. Odijk, *Biophys. J.* **75**, 1223 (1998).
- [10] D. G. Angelescu, R. Bruinsma, and P. Linse, *Phys. Rev. E* **73**, 041921 (2006).

- [11] A. Leforestier, A. Šiber, F. Livolant, and R. Podgornik, *Biophys. J.* **100**, 2209 (2011).
- [12] C. Forrey and M. Muthukumar, *Biophys. J.* **91**, 25 (2006).
- [13] J. Kindt, S. Tzlil, A. Ben-Shaul, and W. M. Gelbart, *Proc. Natl. Acad. Sci. USA* **98**, 13671 (2001).
- [14] P. L. Freddolino, A. S. Arkhipov, S. B. Larson, A. McPherson, and K. Schulten, *Structure* **14**, 437 (2006).
- [15] A. S. Petrov and S. C. Harvey, *Structure* **15**, 21 (2007).
- [16] J. Arsuaga, M. Vázquez, S. Trigueros, D. W. Sumners, and J. Roca, *Proc. Natl. Acad. Sci. USA* **99**, 5373 (2002).
- [17] Y. L. Loo, R. A. Register, and A. J. Ryan, *Phys. Rev. Lett.* **84**, 4120 (2000).
- [18] B. Hornblower, A. Coombs, R. D. Whitaker, A. Kolomeisky, S. J. Picone, A. Meller, and M. Akeson, *Nat. Methods* **4**, 315 (2007).
- [19] M. Bachmann and W. Janke, *Phys. Rev. Lett.* **95**, 058102 (2005); *Phys. Rev. E* **73**, 041802 (2006).
- [20] M. Möddel, W. Janke, and M. Bachmann, *Macromolecules* **44**, 9013 (2011).
- [21] Q. Cao and M. Bachmann, *Soft Matter* **9**, 5087 (2013); *Chem. Phys. Lett.* **586**, 51 (2013).
- [22] A. Šiber, A. Lošdorfer Božič, and R. Podgornik, *Phys. Chem. Chem. Phys.* **14**, 3746 (2012).
- [23] M. Bachmann, *Thermodynamics and Statistical Mechanics of Macromolecular Systems* (Cambridge University Press, New York, 2014).
- [24] G. F. Schneider and C. Dekker, *Nat. Biotechnol.* **30**, 326 (2012).
- [25] H. Salman, D. Zbaida, Y. Rabin, D. Chatenay, and M. Elbaum, *Proc. Natl. Acad. Sci. USA* **98**, 7247 (2001).
- [26] S. M. Simon, C. S. Peskin, and G. F. Oster, *Proc. Natl. Acad. Sci. USA* **89**, 3770 (1992).
- [27] R. Zandi, D. Reguera, J. Rudnick, and W. M. Gelbart, *Proc. Natl. Acad. Sci. USA* **100**, 8649 (2003).
- [28] T. Ambjörnsson and R. Metzler, *Phys. Biol.* **1**, 77 (2004).
- [29] W. Yu and K. Luo, *J. Am. Chem. Soc.* **133**, 13565 (2011).
- [30] I. Ali, D. Marenduzzo, and J. M. Yeomans, *Phys. Rev. Lett.* **96**, 208102 (2006).
- [31] D. G. Angelescu and P. Linse, *Phys. Rev. E* **75**, 051905 (2007).
- [32] H. Arkin and W. Janke, *J. Phys. Chem. B* **116**, 10379 (2012); *Phys. Rev. E* **85**, 051802 (2012).
- [33] K. Kremer and G. S. Grest, *J. Chem. Phys.* **92**, 5057 (1990).
- [34] R. W. Hockney and J. W. Eastwood, *Computer Simulation Using Particles* (Adam Hilger, Bristol, 1988).
- [35] S. Plimpton, *J. Comput. Phys.* **117**, 1 (1995).
- [36] G. S. Grest and K. Kremer, *Phys. Rev. A* **33**, 3628 (1986).
- [37] See Supplemental Material at <http://link.aps.org/supplemental/10.1103/PhysRevE.90.060601> for the discussion of the dynamics and concentration of the polyelectrolyte and the counterions, as well as for the analysis of energies and forces upon successful polyelectrolyte intrusion.
- [38] O. V. Krasilnikov, C. G. Rodrigues, and S. M. Bezrukov, *Phys. Rev. Lett.* **97**, 018301 (2006).
- [39] Q. Cao and M. Bachmann (unpublished).